

Article

New Insights into Synthetic Copper Greens: The Search for Specific Signatures by Raman and Infrared Spectroscopy for Their Characterization in Medieval Artworks

Juliana Buse^{1,2}, Vanessa Otero¹  and Maria J. Melo^{1,*} 

¹ Department of Conservation and Restoration and LAQV-REQUIMTE, NOVA School of Sciences and Technology of NOVA University Lisbon, 2829-516 Monte da Caparica, Portugal; ju.buse@gmail.com (J.B.); van_otero@campus.fct.unl.pt (V.O.)

² Department of Information Sciences, Federal University of Ceará, Fortaleza CEP 60020-181, Brazil

* Correspondence: mjm@fct.unl.pt

Received: 16 April 2019; Accepted: 23 May 2019; Published: 4 June 2019



Abstract: A systematic investigation of medieval copper green pigments was carried out based on written sources: 21 manuscripts, dating from 50–70 to 1755 AD, were sourced and 77 recipes were selected, translating into 44 experiments. Reconstructions from medieval recipes were prepared and characterized through a multianalytical approach to disclose the original pigment formulation that is often described as *verdigris*. Based on the results obtained, we propose three main groups of copper green pigments, *group 1*, in which only $\text{Cu}(\text{CH}_3\text{COO})_2 \cdot \text{H}_2\text{O}$ is formed; *group 2*, where this acetate is found together with copper oxalates; *group 3*, in which atacamite is present as the major green component or as a signature compound. The products formed are in perfect agreement with that predicted by the state-of-the-art research on the mechanisms of atmospheric corrosion of copper. This knowledge, together with our experience on craft recipes to prepare medieval paint materials, allowed us to recover a lost medieval recipe to produce a copper green pigment based mainly on atacamite, a basic copper chloride, which has been recently detected, by Raman and infrared spectroscopy, in artworks ranging from Catalonia and the Crown of Aragon panel painting to Islamic manuscripts.

Keywords: copper green pigments; medieval pigments; conservation; Raman microscopy; infrared spectroscopy

1. Introduction

1.1. Medieval Copper Greens

Copper greens were used as pigments since antiquity until the discovery and dissemination of viridian green, a chromium oxide, in the 19th century [1–5]. Except for malachite, a basic copper carbonate available as a mineral, all the other copper green pigments may have been synthesized during the medieval period as will be discussed in this paper. The medieval artefacts, in which synthetic copper greens have been detected, range from artistic to technical, such as manuscript illuminations and maps. Amid the synthetic copper greens, “copper resinates” and “verdigris” are still the best known medieval copper greens [1,4–7]; as we will show in this work, the main pigment obtained reproducing the medieval process for making *verdigris* is a neutral acetate of copper (Figure 1). More recently, using an analytical approach similar to ours, other copper pigments have been characterized in medieval artworks, such as basic copper sulfates in medieval illuminated manuscripts dated from the 15th century by Eremin et al. [8,9]; basic copper acetates admixed with chlorides as well as oxalates,

also from the 15th century, in Catalonia and the Crown of Aragon paintings (oil and tempera paintings) by Salvadó et al. [10,11]. In this latter work, the authors are uncertain on the origin of these green compounds, in particular, the copper oxalates: Were they applied as synthetic pigments or were they formed due to paint degradation? Eremin et al. [12], in a systematic study on the materials and techniques of Islamic manuscripts, described a variety of mixtures of copper greens to produce subtle variations in color; they detected all the above described compounds and atacamite alone. These authors also discuss the provenance of these greens, either produced artificially as copper corrosion products or as “natural mixtures resulting from use of different ores.” The main analytical techniques used by Salvadó were X-ray diffraction (XRD), X-ray fluorescence (XRF) and infrared spectroscopy; whereas Eremin’s analyses were based on Raman microscopy and XRF (infrared spectroscopy was also used, but with no conclusive identification). Previously published works on the identification of copper greens such as atacamite in paintings were carried out by Naumova, Pisareva and Nechiporenko in the 1990s; the characterization was essentially based on transmitted light microscopy [13,14], and only for a basic copper sulfate found in 16th century Russian frescoes were the XRD data presented.

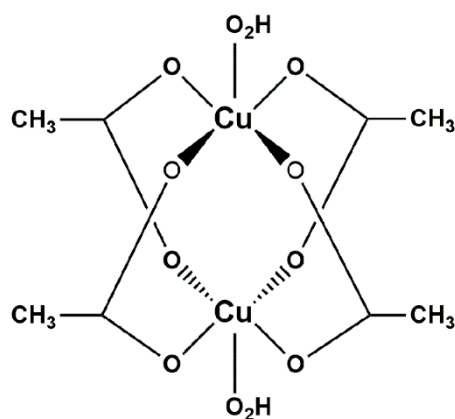


Figure 1. $\text{Cu}(\text{CH}_3\text{COO})_2 \cdot \text{H}_2\text{O}$ represents a bridged carboxylate Cu^{2+} complex.

In what concerns the conservation of this cultural heritage, the use of verdigris on paper raises great concern since its degradation corrodes the organic support, similarly to iron gall inks. Additionally, the changes in color from green to dark brown greatly affect our perception of the artworks [15]. While there has been much research on treatments for stabilizing iron gall inks’ degradation [16], there is still much to be learned on copper acetate degradation [15,17,18].

With this issue in mind, for this work, we systematically synthesized medieval copper green pigments based on written sources (treatises and other technical documents) (Table S1). Twenty-one pre-, post- and medieval manuscripts, dating from 50–70 to 1755 AD, were sourced and 77 recipes were selected to be reproduced, that translated into 44 experiments. The pigments obtained were characterized through a multianalytical approach using Raman microscopy (μRaman), Fourier-transform infrared microspectroscopy (μFTIR), X-ray fluorescence microspectroscopy (μXRF) and X-ray diffraction (XRD). Raman microscopy and infrared spectroscopy were fundamental to fingerprint signature compounds for the three main groups we propose to be representative of medieval copper greens, as will be discussed in this work (Figure S1).

1.2. The Synthesis of $\text{Cu}(\text{CH}_3\text{COO})_2 \cdot \text{H}_2\text{O}$ Using Copper in the Presence of Acetic Acid

In the recipes that were selected for this study, the preparation of $\text{Cu}(\text{CH}_3\text{COO})_2 \cdot \text{H}_2\text{O}$ (Figure 1) is usually made from copper sheets in the presence of, but not in contact with, a source of acetic acid, such as vinegar in a well-sealed container. Thus, the formation of medieval verdigris can be described as a complex atmospheric corrosion process that “incorporates a wide spectrum of chemical,

electrochemical and physical processes in the interfacial domain from the gaseous phase to the liquid phase to the solid phase" [19].

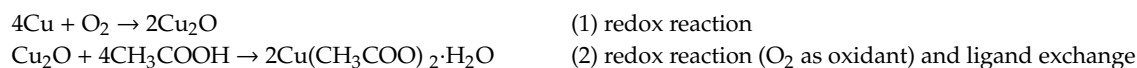
Advances in the understanding of these complex reactions offer a general description of this corrosion process that initiates with the formation of an aqueous adlayer at the copper surface where an oxide layer (thickness of a few nanometers) is formed; usually, it terminates with surface hydroxyl groups next to the liquid layer [19]. This aqueous adlayer results from the instant reaction of water vapor with the metal. Leygraf et al. propose that these hydroxyl groups, next to the liquid layer, may be easily exchanged by other anions and protonated, promoting metal dissolution from the surface [19].

In our experimental conditions, cuprite, copper(I) oxide, is expected to be the initial surface component formed on copper upon atmospheric exposure. Cuprite is formed within the first hours of exposure and continues to grow until developing a copper oxide surface that terminates with hydroxyl groups next to the liquid layer. In a second stage [19–23], acetate ions or protons will promote the dissolution of the metal and the formation of metal-ligand precipitates. Following the formation of the first copper oxide and hydroxide layer, Leygraf et al. propose two reaction pathways: (1) One that involves proton-induced dissolution of cuprous ions and formation of further cuprite, Cu_2O (*pathway 1*, promoted by hydroxyl protonation); (2) another pathway based on ligand-induced dissolution of the cuprous ions and release of an aqueous copper carboxylate species from the surface and their subsequent precipitation as copper(II) acetate (*pathway 2*, promoted by hydroxyl-carboxylate exchange). It was also verified that stronger organic acids, which produce higher concentrations of carboxylate ions, will stimulate *pathway 2*; this was exemplified when comparing the corrosion effect of formic acid and acetic acid: It was observed that formic acid stimulates higher rates of carboxylate-induced dissolution [19,22].

On the other hand, the results obtained by López-Delgado et al. for cuprite, point to a ligand exchange of O^{2-} by CH_3COO^- , possibly due to the higher concentration of the latter [18,19]. These authors also described the formation of basic copper acetates with formula estimated to be " $\text{Cu}_4(\text{OH})(\text{CH}_3\text{COO})_7 \cdot 2\text{H}_2\text{O}$ ", because of its assumed structural similarity to $\text{Co}_4(\text{OH})(\text{CH}_3\text{COO})_7 \cdot 2\text{H}_2\text{O}$, based on comparable XRD patterns [20,21].

In the final stages, with prolonged exposure, the number of precipitated nuclei and their sizes increase until eventually they completely cover the metal surface—at this stage they are described as corrosion products. Besides Cu_2O , common corrosion products that have been identified within the patina are; (1) on copper in *SO₂/sulfate-dominated environments*, basic copper sulfates such as posnjakite ($\text{CuSO}_4 \cdot 3\text{Cu}(\text{OH})_2 \cdot \text{H}_2\text{O}$), brochantite ($\text{CuSO}_4 \cdot 3\text{Cu}(\text{OH})_2$) and antlerite ($\text{CuSO}_4 \cdot 2\text{Cu}(\text{OH})_2$); (2) on copper in *chloride-dominated environments*, paratacamite ($\text{Cu}_2(\text{OH})_3\text{Cl}$), atacamite ($\text{Cu}_2(\text{OH})_3\text{Cl}$) and its isomorphous compounds [19,24]. Recent findings have also identified nantokite (CuCl) within the patina at marine conditions with high chloride-deposition rates [19,23].

Based on the experimental results and findings of these two groups, we propose the following global reactions to produce *verdigris*, in *acetate-dominated environments*, as described in medieval recipes [19–22]:



1.3. Characterizing Verdigris and Other Copper Patinas by Raman Spectroscopy

Copper acetates, such as $\text{Cu}(\text{CH}_3\text{COO})_2 \cdot \text{H}_2\text{O}$ in Figure 1, are characterized by Raman through the bands assigned to the acetate group, namely at 703 cm^{-1} attributed to the OCO bend, 948 cm^{-1} due to CC stretch (strong intensity), 1418 cm^{-1} due to the CH_3 bend, 1440 cm^{-1} due to the stretch of the COO group, 2941 , 2989 and 3024 cm^{-1} attributed to CH stretches. A strong band is also observed at 322 cm^{-1} , which together with the band at 231 cm^{-1} may be assigned to Cu-O stretches [25–27]. San Andrés et al. and Coccato et al. have also identified other copper pigments by Raman spectroscopy [28,29]. Coccato et al. have made available a comprehensive set of Raman spectra for sulfates, antlerite ($\text{CuSO}_4 \cdot 2\text{Cu}(\text{OH})_2$), brochantite ($\text{CuSO}_4 \cdot 3\text{Cu}(\text{OH})_2$), posnjakite ($\text{CuSO}_4 \cdot 3\text{Cu}(\text{OH})_2 \cdot \text{H}_2\text{O}$) and langite

($\text{CuSO}_4 \cdot 3\text{Cu}(\text{OH})_2 \cdot 2\text{H}_2\text{O}$), as well as chlorides, atacamite, paratacamite, clinoatacamite and botallackite ($\text{Cu}_2(\text{OH})_3\text{Cl}$) [29]. Frost et al., based on Raman spectroscopy, proposed that clinoatacamite and botallackite are polymorphs of atacamite, but paratacamite is a “separate mineral with a different structure,” displaying different Raman spectra that allow for a straightforward distinction in the O-H region [24]. The copper sulfates are easily distinguished due to the strong band for the sulfate symmetric stretch around 970 and 990 cm^{-1} and the OH stretch region around 3600 and 3200 cm^{-1} [29–31]. On the other hand, copper chlorides are identified by the bands below 600 cm^{-1} assigned to O-Cu-O and Cl-Cu-Cl modes, the bands between 800 and 1000 cm^{-1} attributed to Cu-OH and OH bends and most importantly by the strong intensity of the OH stretch region around 3600 and 3200 cm^{-1} [8,24,29]. Copper oxalates ($\text{CuC}_2\text{O}_4 \cdot n\text{H}_2\text{O}$) have also been identified by Raman and are mainly characterized by an intense band at 1518 cm^{-1} with a shoulder at 1486 cm^{-1} due to CO stretches, in addition to intense bands at 556 and 209 cm^{-1} assigned to the Cu-O stretches [32–34].

1.4. Characterizing Verdigris and Other Copper Patinas by Infrared Spectroscopy

Neutral copper acetate is characterized by medium-strong infrared peaks at 3476, 3374 and 3272 cm^{-1} corresponding to the OH stretching modes of the water molecule associated to the acetate ion [27]. The weak bands at 2988 and 2941 cm^{-1} , common in spectra of acetates in general, correspond to the asymmetric and symmetric CH stretching modes, respectively [35]. In the fingerprint region, the main bands are: the strong stretching absorption of the COO^- group at 1602 cm^{-1} ; the absorption at 1445 cm^{-1} assigned to CH_3 asymmetric bending, with a shoulder at 1421 cm^{-1} assigned to the symmetric stretching mode of the COO^- group [11,12,27,35,36].

Salvadó et al. have detected basic copper chlorides in historical green paints through their characteristic infrared bands at 3341 and 3443 cm^{-1} (strong intensity) together with a set of weak intensity bands in the region 800–100 cm^{-1} assigned to OH stretches and bendings, respectively [10,11].

Copper oxalates have been mostly associated to degradation products and their identification is based on the asymmetric stretching mode of the COO^- group at 1677 cm^{-1} and the symmetric stretching and bending modes of the COO^- group at 1364 and 1320 cm^{-1} [11,32,37–39].

2. Experimental

2.1. Materials

2.1.1. Reference Materials

Neutral copper acetate monohydrate ($\text{Cu}(\text{CH}_3\text{COO})_2 \cdot \text{H}_2\text{O}$) used in this work was from Kremer and copper oxalate ($\text{CuC}_2\text{O}_4 \cdot n\text{H}_2\text{O}$) from Alfa Aesar. The reference for atacamite ($\text{Cu}_2(\text{OH})_3\text{Cl}$) was of mineral source from Burra, Australia (kindly provided by Geoscience Museum at Instituto Superior Técnico, Lisbon), and cuprite (Cu_2O) was prepared as a copper patina at the Department of Conservation and Restoration by Sara Fragoso (NOVA School of Sciences and Technology).

2.1.2. Ingredients

The two main ingredients were a source of copper (Cu) and a source of acetic acid (CH_3COOH). Metallic copper foils, 99.9% in Cu, with a thickness of ca. 0.8 mm, were cut in 9 cm × 2 cm sheets, hand polished (sandpaper no. 220). Brass 0.5-mm sheets were also used, with equivalent metal purity and a 2:1 Cu/Zn ratio. Copper and brass foils were acquired at Francisco Soares Lda. (Carnaxide, Portugal).

For the acetic acid sources, two different kinds of vinegar were used: A commercial white wine vinegar (Auchan, Portugal), with 6% acidity and a pH 2.5, and a handmade red wine vinegar, pH 3.0, made in the Serra da Estrela region (Portugal) which was aged for roughly one year in oak barrel. Before using, both vinegars were previously heated at 70 °C, as suggested in some recipes. This will be further discussed in the Results and Discussion.

The additives used are next described.

A first subset is made of salts. Recipes mention “salt,” “common salt” or seldom “sea salt”, which were all taken as synonyms meaning sea salt—not pure sodium chloride (NaCl), as sodium (Na⁺) and chlorine (Cl⁻) ions only respond for 85.62% of sea salt’s solid residue, with sulfate (SO₄⁻²) and magnesium (Mg⁺²) responsible for 11.36% and so on [40]. Commercial, additive-free, nonpurified, coarse sea salt (Vatel, Portugal) was acquired and ground by hand in agate mortar. Alternatively, some recipes recommend using salt that was first “calcined,” which led us to submitting some of the above-mentioned hand-ground sea salt to a calcination procedure, in accordance with Theophilus’ recommendations, which read: “[. . .] take a flat pan full of salt and, pressing the salt down firmly, put the pan in the fire and cover it with [glowing] coals for the night. Next morning grind the salt very carefully on a dry stone [41].” We did not use coal, but a gas-fired heated steel pan. For alum, either referred to as simply “alum” or as “Yemeni alum,” reagent-grade potassium alum was used, i.e., aluminum potassium sulfate dodecahydrate (KAl(SO₄)₂·12H₂O). Likewise for “sal ammoniac”, for which reagent grade ammonium chloride (NH₄Cl) was used.

Honey is prescribed in many recipes and we always used it from a single “mel de urze” batch, a common Portuguese name for plants of the *Ericaceae* family, harvested at Concelho de Vila Pouca de Aguiar (Trás-os-Montes, Portugal). Parchment glue was tested as a substitution of honey (for more details on this choice, please see Section 2.2. and Results and Discussion). It was prepared with goat parchment, acquired from the *Musée du Parchemin* (France), following the procedure described in “The Book of How to Make Colors” (*O livro de como se fazem as cores*) [42]; the parchment was washed with distilled water, cut in small pieces (~0.5 cm × 0.5 cm), which were then put in a beaker and it was filled with distilled water (relative initial amounts, 1 g parchment: 10 ml distilled water). The beaker was coated and covered with aluminum foil, so that heating was uniform at 70–80 °C. It was then uncovered for allowing some evaporation, then more distilled water was added and again covered, maintaining the heating; this was repeated until the glue was concentrated, whose texture and viscosity were tested with fingers (as indicated in the recipe). The pieces of parchment were removed and the glue was kept in the refrigerator.

The last additive is soap, which was commercially acquired (blue and white traditional *Offenbach* Portuguese soap, Confiança, Portugal; if dissolved in water it produces strongly alkaline solutions, pH 11).

Millipore water was used in all the experiments.

2.2. Preparation of Medieval Copper Greens

Experiments were carried out in closed containers made of glass and oak. Whenever the recipe mentioned oak or simply wood, we used custom made white oak (*Quercus alba*, imported from the United States) boxes, measuring (internally) 24 cm wide × 14 cm deep × 18 cm high, and, for the one experiment using horse dung, a box measuring (internally) 8 cm wide × 8 cm deep × 11 cm high, always ~5 mm thick, with superior dovetail cover, no hinges, no varnish or any other coating. It was hand-made in a carpentry workshop. Oak boxes had two tiny hooks bolted externally (without reaching the interior) on each of the smaller sides, so that nylon threads could be tied longways across the opening and thus used to suspend copper or brass sheets. Glass vessels, 16.5 cm high × 12 cm diameter (volume 1 L), had a natural rubber pressure hermetic seal lid.

Based on the experimental results obtained, we describe the three types of recipes which might be taken as representative of the three main groups of copper greens we have characterized, Figure 2.

Group 1: “Spanish green” in recipe § 1.16.5 of the “Montpellier manuscript” (*Liber diversarum arcium*) [43], seen identically in an equally named recipe of Theophilus’ *Schedula diversarum atrium* [41]:

“Preparation. If, then, you want to prepare or make Spanish green, take thinned tablets of copper and rasp them carefully on both sides, and pour hot pure vinegar over them, without honey and salt, and put them together in that wood [container] or vessel, not touching the vinegar, and after two weeks check, and scrape; and do thus until it will suffice you [43].”

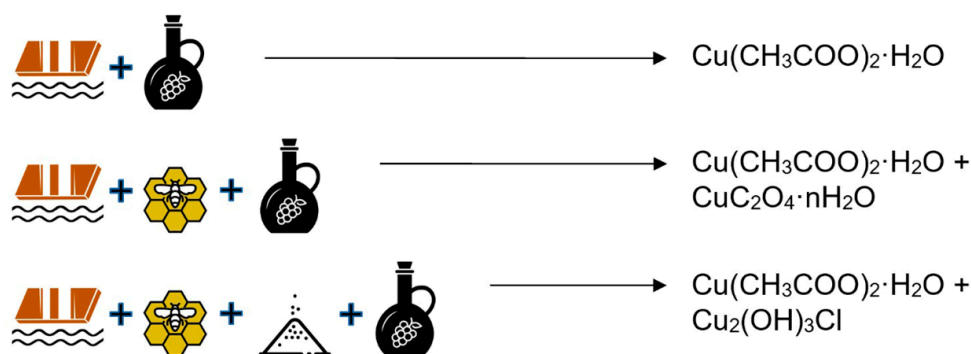


Figure 2. Scheme of the ingredients and final products of representative recipes for groups 1, 2 and 3.

Vinegar of commercial and handmade source, 20 to 40 mL, was always filtered and heated to $\sim 70^\circ\text{C}$, and then poured in Petri dishes or beakers placed inside the oak box. The (copper or brass) sheets were bent 90° downwards at ~ 0.5 cm from the edge parallel to the smaller sides. These bends were used to secure the sheets while suspended by the nylon cord hanging longways attached to the external hooks. Each sheet was put directly above a Petri dish (or beaker), with usually four dishes and four sheets per box. After the time indicated in the recipe, the box was opened and the sheets were scraped for retrieving the pigment produced.

Variations included using a glass container, and replenishing the dish(es) with vinegar and again closing the vessel for additional time.

Glass vessels were used similarly, but with a single sheet and dish. Sheet suspension was achieved similarly: Nylon cord was tied to the hinges and to the glass lid metal frame.

Group 2: Recipe § 130 of the Paduan manuscript (*Ricette per far ogni sorte di colori*) [44]:

“To make verdigris.—Take pieces of copper anointed with purified honey, and fasten them to the cover of a well-glazed pipkin, which must be full of hot vinegar made with strong wine; then cover it and place it in a warm situation for 4 or 5 weeks, and when you uncover it, remove the colour which you will find on the pieces of copper, and it will be most beautiful [44].”

A thin layer of honey was applied to both sides of the sheets with a paint brush. Interestingly, too much honey proved to entirely prevent the sheet corrosion.

This recipe was tested for honey’s substitution by parchment glue, in order to evaluate whether its role is of a chemical nature or rather simply hygroscopic.

Group 3: Recipe § III.XXXVIII of Eraclius’ and pseudo-Eraclius’ *De coloribus et artibus romanorum* (8th–13th centuries; as the recipe belongs to the third part, its specific authorship is ascribed to “pseudo-Eraclius”) [44]:

“How to make a green colour from salt.—I have often mentioned a green colour, and now I will tell you how I make it. I take a piece of oak, of whatever length and breadth I please, and scoop it out into the shape of a scrinium. I then take copper, and cause it to be hammered out into plates as long as I choose; that is, so that their length may cover the breadth of the hollow wood. Afterwards I take a ladleful of salt, and pressing it strongly down, I put it into the fire for a night, and cover it up with coals; and the next day grind it very carefully upon a dry stone. I then take small twigs, and place them in the aforesaid wood, so that two parts of the hollow wood may be underneath and the third above. Then smearing the copper-plates on both sides with honey, I sprinkle the salt all over the honey, then shake the plates over the ladle to avoid waste, and then place the plates upon the twigs. I next cover up the hollow wood with another piece made for this purpose, and lute it all round with clay well mixed with asses’ dung. But before I cover up the hollow wood, I pour into it hot vinegar or hot urine, so as to fill one-third part of it, and then cover it up, and afterwards do as before directed with this colour [44].”

The addition of ~1–2 g of sea salt, duly weighed, was manually sprinkled. Too much sea salt resulted in a strong corrosion environment, which led to the sheet breaking in two and thus falling into the vinegar-filled dish, which hinders the ulterior pigment extraction.

This recipe was also tested for honey's substitution by parchment glue, evaluating not only its hygroscopic role but also its role in chloride diffusion.

2.3. Equipment and Characterization Methods

2.3.1. Raman Microscopy (μ Raman)

Raman microscopy was carried out using a Labram 300 Jobin Yvon spectrometer, equipped with a HeNe laser 17 mW operating at 632.8 nm and a solid state laser operating at 532 nm. Spectra were recorded as an extended scan. The laser beam was focused with a 50 \times or a 100 \times Olympus objective lens. The laser power at the surface of the samples was controlled with the aid of a set of neutral density filters (optical densities 0.3, 0.6). The system was calibrated using a silicon standard. Raman data analysis was performed using LabSpec 5 software. All spectra are presented as acquired without any baseline correction or other treatment.

2.3.2. Fourier Transform Infrared Microspectroscopy (μ FTIR)

Infrared analyses were performed using a Nicolet Nexus spectrophotometer coupled to a Continuum microscope (15 \times objective) with a MCT-A detector cooled by liquid nitrogen. The pigments were prepared as KBr pellets or compressed in a diamond anvil cell. For pellets, spectra were collected in transmission mode, from 4000 to 400 cm^{-1} , with a resolution of 4 cm^{-1} and 64 scans. For microsamples, spectra were collected from 4000 to 650 cm^{-1} , with a resolution of 4 or 8 cm^{-1} and 128 scans. Omnic E.S.P. 5.2 software was used to perform the spectral analysis. The spectra are shown here as acquired, without corrections or any further manipulations, except for the occasional removal of the CO_2 absorption at ca. 2300–2400 cm^{-1} .

2.3.3. Micro-Energy Dispersive X-ray Fluorescence (μ -EDXRF)

Micro-EDXRF spectra were obtained with an ArtTAX spectrometer of Intax GmbH, with a molybdenum (Mo) anode, Xflash detector refrigerated by the Peltier effect (Sidrift), with a mobile arm. The spatial resolution is 70 μm . The experimental parameters used were: 40 kV of voltage, 400 μA of intensity and 300 s of acquisition time, under helium gas flux.

2.3.4. X-Ray Diffraction (XRD)

X-ray diffraction patterns were acquired with a RIGAKU X-ray diffractometer MiniFlex II using CuK α radiation (30 kV and 15 mA) in the $10 < 2\theta < 80$ range with a 1 $^\circ$ step size, at the LAQV-REQUIMTE Analysis Laboratory (FCT NOVA). The ICDD PDF-2 reference database (2007) was used to interpret the XRD patterns.

3. Results and Discussion

3.1. Characterization of the Synthesized Pigments

Forty-four syntheses of verdigris were carried out, 26 in glass vessels and 18 in oak boxes (Table 1 and Table S1). The results of these experiments could be assembled in five groups (Table 1 and Figure S1). Excepting for two processes that are included in group 4, $\text{Cu}(\text{CH}_3\text{COO})_2 \cdot \text{H}_2\text{O}$ was always produced, as predicted (Figures 3–5 and S2).

In group 1, only $\text{Cu}(\text{CH}_3\text{COO})_2 \cdot \text{H}_2\text{O}$ was synthesized (Figure 3 and Figure S2). However, two important classes of other copper compounds could also be found together with $\text{Cu}(\text{CH}_3\text{COO})_2 \cdot \text{H}_2\text{O}$: Copper oxalates (group 2) and basic copper chlorides (group 3) (Figures 4 and 5). Their importance as Raman and infrared markers will be discussed in the next sections (Tables 2 and 3).

Table 1. The 44 experiments to produce synthetic copper greens were carried out in close containers; 26 were carried out in a glass vessel and 18 in oak boxes. The main products formed are assembled in three main groups; the number of experiments that lead to their formation is reported together with its value in % (for more details please see text).

Reaction Vessel	Group 1 $\text{Cu}(\text{CH}_3\text{COO})_2 \cdot \text{H}_2\text{O}$	Group 2 [§] $\text{Cu}(\text{CH}_3\text{COO})_2 \cdot \text{H}_2\text{O}$ $\text{Cu}_2\text{O}_4 \cdot n\text{H}_2\text{O}$	Group 3 $\text{Cu}(\text{CH}_3\text{COO})_2 \cdot \text{H}_2\text{O}$ $\text{Cu}_2(\text{OH})_3\text{Cl}$ CuCl	Group 4 miscellaneous	Group 5 no products
glass vessel 	6 13.6%	6 13.6%	1 2.3%	2 4.5%	11 25%
oak box 	7 15.9%	3 6.8%	5 11.4%	1 2.3%	2 4.5%

[§] Other compounds were found in two processes, sodium oxalate and zinc acetate.

In *group 2*, copper oxalate was always found, and occasionally sodium oxalate was detected, in minor amounts¹ (Figure 4).

Group 3 displayed a more complex signature (Figure 5 and Figure S2B). We detected the presence of atacamite, which is in agreement with what is described in the literature for common patina constituents on copper, formed in chloride-dominated environments. Nantokite (CuCl), which has been recently identified within the patina at marine conditions with high chloride deposition rates [19,23], was tentatively identified as a minor compound by the peak at 1100 cm^{-1} in the infrared spectrum; the high Cl^- mobility may have been possible due to the presence of honey, but also with parchment glue, a tested substitution. Ammineite ($\text{CuCl}_2(\text{NH}_3)_2$) was also detected as an intermediate. It is an unstable compound that when exposed to the atmosphere converts into a copper chloride (Figure S3) [45].

It is very interesting to note that the percentage of unsuccessful syntheses was much higher for the glass vessel (25%) compared to the wooden box (4.5%), indicating that the volatiles released by the oak box play an important role in initiating the reaction [19]. It is also worth noting that all recipes were prepared using vinegar previously heated at ca. 70°C ; this was suggested in some recipes and it was included in all experiments as we observed that better yields were usually obtained with this procedure.

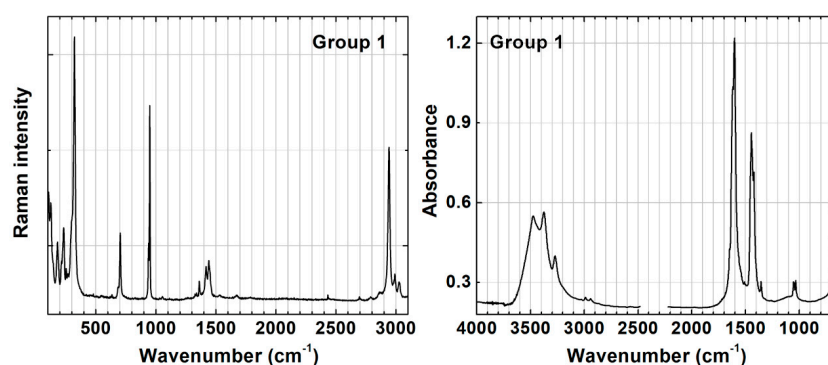


Figure 3. Representative Raman and infrared spectra for group 1, from recipes characterized by producing only $\text{Cu}(\text{CH}_3\text{COO})_2 \cdot \text{H}_2\text{O}$; these infrared and Raman spectra may be considered as references for $\text{Cu}(\text{CH}_3\text{COO})_2 \cdot \text{H}_2\text{O}$.

¹ In a recipe using brass in an oak box, we also detected the presence of zinc acetate, in agreement with the literature [17].

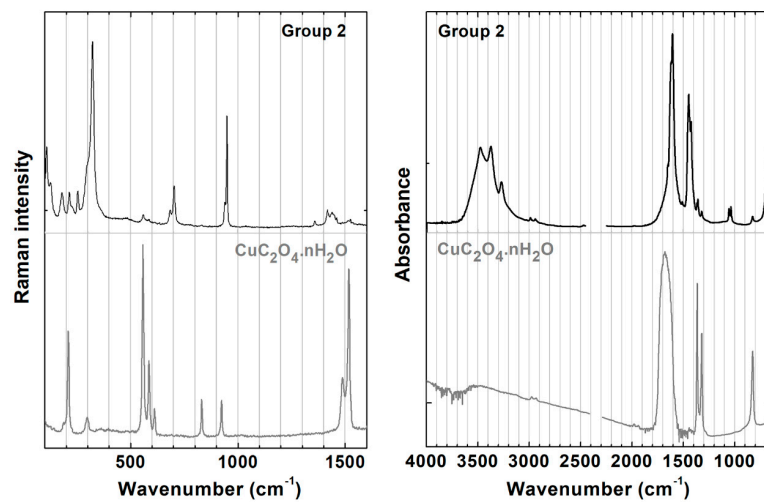


Figure 4. Representative Raman and infrared spectra for group 2, which is characterized by the signature compound $\text{CuC}_2\text{O}_4 \cdot n\text{H}_2\text{O}$ together with the $\text{Cu}(\text{CH}_3\text{COO})_2 \cdot \text{H}_2\text{O}$ (main compound). Reference Raman and infrared spectra for copper oxalate are shown in grey, below.

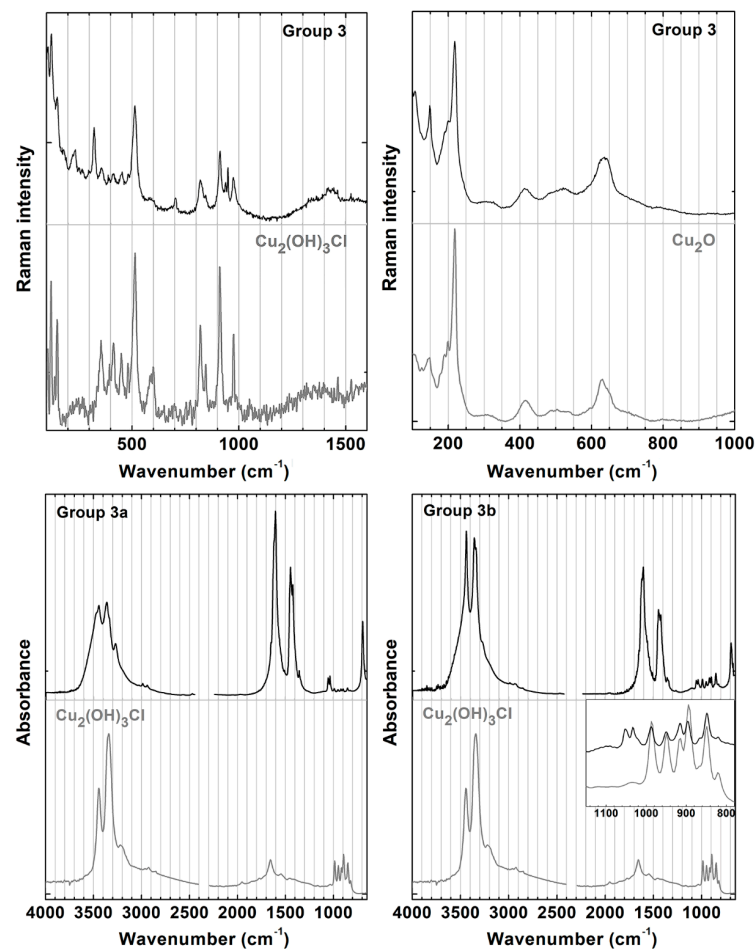


Figure 5. Raman and infrared spectra of group 3, in which atacamite $\text{Cu}_2(\text{OH})_3\text{Cl}$ may be present as a minor component together with the $\text{Cu}(\text{CH}_3\text{COO})_2 \cdot \text{H}_2\text{O}$, group 3a, or as a major compound, group 3b; Cu_2O was also detected by Raman. Reference Raman and infrared spectra for a mineral sample of atacamite and Cu_2O are shown in grey, below.

3.2. Detailed Characterization of Groups 1 and 2

As mentioned, pigments in *group 1* are characterized solely by copper(II) acetate monohydrate ($\text{Cu}(\text{CH}_3\text{COO})_2 \cdot \text{H}_2\text{O}$). μ -EDXRF shows a high intensity signal for copper only. The infrared spectrum of neutral copper acetate monohydrate produced according to medieval recipes, Figure 3, matches the spectrum of modern pure commercial samples of the compound [46]. This was also observed by Salvadó et al. and San Andrés et al. [5,11].

In *group 2*, together with $\text{Cu}(\text{CH}_3\text{COO})_2 \cdot \text{H}_2\text{O}$ we found copper oxalate as a minor compound, as may be observed in the infrared spectrum, Figure 4. The infrared signature bands for copper oxalate are observed at 1364 and 1320 cm^{-1} (COO^- stretching and OCO bending) together with a band at 824 cm^{-1} (CC stretching); its presence was unequivocally confirmed by Raman microscopy through the bands at 556 cm^{-1} (CuO stretching) and 1518 cm^{-1} (CO stretching), Figure 4 and Table 2 [32,47–51].

Table 2. Main Raman characteristic bands (cm^{-1})* for the synthesized compounds: copper acetate monohydrate ($\text{Cu}(\text{CH}_3\text{COO})_2 \cdot \text{H}_2\text{O}$), copper oxalate ($\text{CuC}_2\text{O}_4 \cdot n\text{H}_2\text{O}$), basic copper chloride ($\text{Cu}_2(\text{OH})_3\text{Cl}$) and copper(II) oxide (Cu_2O).

Copper Acetate $\text{Cu}(\text{CH}_3\text{COO})_2 \cdot \text{H}_2\text{O}$			Copper Oxalate $\text{CuC}_2\text{O}_4 \cdot n\text{H}_2\text{O}$			Basic Copper Chloride $\text{Cu}_2(\text{OH})_3\text{Cl}$			Copper(II) Oxide Cu_2O		
231	m	$\nu(\text{CuO})$	209	m	$\nu(\text{CuO})$	119	w		218	vs	$\nu(\text{CuO})$
322	vs		556	vs		147	w	$\delta(\text{OCuO})$	418	w	
703	m	$\delta(\text{OCO})$	585, 610	sh		513	w	$\nu(\text{CuO})$	630	w	
948	s	$\nu(\text{CC})$	831	m	$\delta(\text{OCO})$	911	w	$\delta(\text{CuOH})$			
1418	sh	$\delta(\text{CH}_3)$	924	m	$\nu(\text{CC})$	3329	w	$\nu(\text{OH})$			
1440	m	$\nu(\text{COO}^-)$	1486	sh	$\nu(\text{CO})$	3350	m				
2941	s	$\nu(\text{CH})$	1518	s		3435	vs				
2989, 3024	sh		1615	w							

* w—weak, m—medium, s—strong, vs—very strong, sh—shoulder.

3.3. Detailed Characterization of Group 3

All samples in *group 3* resulted from recipes that used sea salt, either raw or calcined, except for one sample where sal ammoniac was used. It was possible to detect the presence of Cl by μ -EDXRF. Infrared spectroscopy allowed us to provide a semiquantitative analyses of copper(II) acetate monohydrate and atacamite by comparison with reference compounds, Figure 5. Basic copper chlorides may be found in higher concentration than $\text{Cu}(\text{CH}_3\text{COO})_2 \cdot \text{H}_2\text{O}$ (*group 3b*), but they can also be found as a minor component in the overall pigment composition (*group 3a*). As mentioned above, basic copper chlorides are straightforwardly identified by their weak but very well resolved bands attributed to OH bending modes in the 1000 – 800 cm^{-1} region, namely at 986 , 949 , 894 and 849 cm^{-1} (inset in Figure 5), as well as by their high absorption bands resulting from the OH stretching modes at 3443 and 3341 cm^{-1} . They match very well the bands of synthetic atacamite reported by Martens et al. at 987 , 950 , 915 , 896 , 850 and 819 cm^{-1} [52] and by Frost et al., 984 , 944 , 913 , 890 , 869 , 844 and 820 cm^{-1} [24]. However, it is also close to the basic copper chloride described by Salvadó et al. as paratacamite at 986 , 949 , 916 , 895 , 850 and 820 cm^{-1} [11]. At the same time, the bands of our infrared spectrum diverge from those of paratacamite and clinoatacamite reported by Frost et al., Martens et al., Braithwaite et al. and Liu et al. and also diverge from botallackite's bands described by Braithwaite et al. and Liu et al. [24,52–55]. The presence of atacamite on the synthesized copper green pigments was confirmed by Raman microscopy and XRD diffraction [56], Figure 5 and Figure S2B, but paratacamite was not detected. This technique also allowed the detection of Cu_2O .

In four of the experiments studied in *group 3*, it was also possible to detect a weak infrared band at 1103 – 1100 cm^{-1} , suggesting the formation of the intermediate compound copper(I) chloride, CuCl , which as a mineral is known as nantokite. This agrees with reports by Banik and Scott et al. [57,58]: Both found CuCl in areas associated with honey when executing the same recipe. What is interesting, though, is that CuCl was formed not only when honey was used but also when it was substituted

by parchment glue. The chemical process by which CuCl may convert into other products is not yet fully understood, but Scott [58] confirmed by XRD its transformation into atacamite when exposed to humidity. It is thus possible that the process of conversion of the small quantity of nantokite into atacamite was in course for the analyzed samples. This seems to confirm the role of honey or parchment glue in promoting the mobility of chloride ions and, therefore, high chloride deposition rates.

Table 3. Main infrared characteristic bands (cm^{-1})* for the synthesized compounds: Copper acetate monohydrate ($\text{Cu}(\text{CH}_3\text{COO})_2 \cdot \text{H}_2\text{O}$), copper oxalate ($\text{CuC}_2\text{O}_4 \cdot n\text{H}_2\text{O}$) and basic copper chloride ($\text{Cu}_2(\text{OH})_3\text{Cl}$).

Copper Acetate $\text{Cu}(\text{CH}_3\text{COO})_2 \cdot \text{H}_2\text{O}$			Copper Oxalate $\text{CuC}_2\text{O}_4 \cdot n\text{H}_2\text{O}$			Basic Copper Chloride $\text{Cu}_2(\text{OH})_3\text{Cl}$		
629	m	$\delta(\text{COO}^-)$	824	<i>m</i>	$\nu(\text{CC})$	849	w	
692	m	$\delta(\text{COO}^-)$	1320	<i>s</i>	$\nu_s(\text{COO}^-)/$	894	w	
1033	w	$\delta(\text{CH}_3)$	1364	<i>s</i>	$\delta(\text{OCO})$	949	w	$\delta(\text{OH})$
1052	w	$\delta(\text{CH}_3)$	1677	<i>vs</i>	$\nu_a(\text{COO}^-)$	986	w	
1445	<i>s</i>	$\delta(\text{CH}_3)$				1655	w	
1602	<i>vs</i>	$\nu(\text{COO}^-)$				3341	<i>vs</i>	$\nu(\text{OH})$
3475, 3375, 3272	<i>m</i>	$\nu(\text{OH})$				3443	sh	

* w—weak, m—medium, s—strong, vs—very strong, sh—shoulder, a—asymmetric, s—symmetric.

3.4. Oxalates as Degradation Products or Markers of Specific Recipes?

The biogenic or chemical origin of oxalates in works of art is still a matter of dispute [59–63]. Nevertheless, the importance of the binder in the formation of oxalates in both tempera and oil paintings is well documented in the literature [61,63], and oxalic acid is generally considered an end-product of the oxidation of more complex carboxylic acids [61]. As to their presence in the original composition of historical pigments, Nevin et al. state that “[...] a copper oxalate has not been identified or analytically documented as an artist’s pigment, nor is it known to have been historically mined or manufactured for use as a material for painting [34].” Nevertheless, our historically accurate reproductions of medieval recipes prove that copper oxalate and other oxalates can be present in the original copper green pigment. This results from the craft nature of medieval pigment production, which used nonpure reagents and selected additives based on a “savoir faire” and craft knowledge now lost. This is very different from the pure, reagent-grade modern ingredients systematically used in studies of artists’ materials.

It should be noted that the identification of oxalates in group 2 does not oppose to the fact that they may be considered as markers of binder degradation in, particularly, calcium oxalate as proposed by several authors [11,61,63–65].

4. Conclusions

Copper green pigment reconstructions from historical recipes were prepared and characterized to know more about the original pigment formulation that is commonly described as *verdigris*. Our results show that the products formed are in perfect agreement with that predicted by the state-of-the-art research on the mechanisms of atmospheric corrosion of metals, in this case, of copper [19,22]. They are also in agreement with studies on patinas [19,24,26,29,30,49,66–69]. Based on the pigments obtained and described in Table 1, we propose three main groups of copper green pigments that in the future may expand with the study of other documentary sources (for example, middle English recipes [70]). Our research confirms that the use of vinegar in a close container will result in the formation of $\text{Cu}(\text{CH}_3\text{COO})_2 \cdot \text{H}_2\text{O}$, a neutral copper acetate. In addition, in a wooden box, in 30% of the experiments, it was the sole green pigment formed, *group 1* (Table 1). It is important to refer that no other form of copper acetates was detected (e.g., basic copper acetates). On the other hand, in 65% of the experiments, our results show that other important green compounds may be formed such as oxalates and chlorides (Table 1). For *group 2*, we highlight that copper oxalate was present in the original pigment formulation,

and, therefore, caution must be taken when considering it a degradation product of the paint color (or the binding medium). In fact, medieval *verdigris* was prepared as a degradation product of copper, so several other corrosion greens should be expected to form in this process. In *group 2* these copper oxalates were detected as minor compounds in formulations in which neutral copper acetate was the major compound, and for this reason we propose that they may be used as signature compounds for the making of *verdigris*; further work will be required to associate it to a specific type of recipe. In the presence of a binder, it will be more difficult to use them as signature compounds, as they may result from the degradation of the binding medium. In the presence of NaCl as an additive, depending on the experimental conditions, basic copper chlorides are formed in variable amounts together with neutral copper acetate. In the experiments in which we used parchment glue as a substitute for honey, we found that atacamite type structures could be formed as the major copper green. In this case, *verdigris* cannot be described as mainly a copper acetate, but as a mixture of atacamite and $\text{Cu}(\text{CH}_3\text{COO})_2 \cdot \text{H}_2\text{O}$; so, atacamite is a marker compound for *group 3*, and may be found as a, minor, signature compound for certain processes (*group 3a*), or it may be the major green pigment (*group 3b*). These findings are in agreement with the characterization of basic copper chlorides in the 15th century Catalonia and the Crown of Aragon paintings (oil and tempera paintings), systematically studied by Salvadó et al. [10,11]. They are also in agreement with what observed by Eremin et al. in a recent study on Islamic manuscripts [12], in which certain shades of green only present atacamite.

Atacamite as the major copper green pigment resulted from a variation of a medieval recipe where honey was substituted by parchment glue. We tested this variation because we know that many craft recipes have not been documented in written sources, but were part of an anonymous craft “savoir faire” that has been lost. It was very exciting to find that this kind of formulation was detected in works of art ranging from panel painting to medieval illuminations, and from Europe to Persia [10–13]. We consider that one of our main contributions lies in the integration of our knowledge on craft recipes that describe the manufacture and preparation of paint materials with the state-of-the-art research on the mechanisms of atmospheric corrosion of metals. By integrating these “two different worlds,” we may have recovered a lost medieval recipe to produce a copper green based in atacamite, a basic copper chloride.

In the future, we will further explore recipes to produce basic copper chlorides as well as sulfates; we will also extend our analytical characterization to include powder diffraction analysis of relatively amorphous compounds using novel approaches [71,72].

Supplementary Materials: The following are available online at <http://www.mdpi.com/2571-9408/2/2/99/s1>, Figure S1: Representative pigments for each group; Figure S2: Representative diffraction patterns of (A) group 1 with the detection of $\text{Cu}(\text{CH}_3\text{COO})_2 \cdot \text{H}_2\text{O}$, (B) group 3 where $\text{Cu}_2(\text{OH})_3\text{Cl}$ (●) was detected together with $\text{Cu}(\text{CH}_3\text{COO})_2 \cdot \text{H}_2\text{O}$; the identification of the copper oxalate was not possible by XRD most probably because it is in an amorphous form; Figure S3: Infrared spectrum of group 3 example where ammineite ($\text{CuCl}_2(\text{NH}_3)_2$) (◆) was detected together with $\text{Cu}(\text{CH}_3\text{COO})_2 \cdot \text{H}_2\text{O}$ and $\text{Cu}_2(\text{OH})_3\text{Cl}$ (●); Table S1: Written sources and specific recipes reproduced, together with a visual summary of the experimental set-up (see caption below the table) and final products. The main products formed are assembled in four groups; group 5 includes recipes in which no pigments were formed (unsuccessful).

Author Contributions: J.B. carried out the investigation of the copper green pigments, having acquired, analyzed and interpreted the data. V.O. acquired and interpreted the spectral data. M.J.M. supervised the research work and contributed with the conception and design of the manuscript; she also acquired and interpreted the spectral data. All authors contributed to the writing and revision of the manuscript. All authors read and approved the final manuscript.

Funding: This research was funded by Fundação para a Ciência e Tecnologia, Ministério da Educação e da Ciência (FCT/MCTES), Portugal, through doctoral programme CORES-PD/00253/2012; Associated Laboratory for Green Chemistry–LAQV, financed by FCT/MCTES (UID/QUI/50006/2019); and Coordenação de Aperfeiçoamento de Pessoal de Nível Superior, Ministério da Educação (CAPES/MEC), Brazil, Finance Code 001, through doctoral programme Ciências sem Fronteiras.

Acknowledgments: The authors would like to thank Mark Clarke for sharing his invaluable knowledge and scholarship on medieval written sources and for his continuous support and helpful discussions. Amélia Dionísio and Sara Fragoso are gratefully acknowledge for giving us access to reference samples.

Conflicts of Interest: The authors declare no conflict of interest.

References

1. Kühn, H. *Artists' Pigments: A Handbook of Their History and Characteristics*; Ashok, R., Ed.; National Gallery of Art: Washington, DC, USA; Oxford University Press: Oxford, UK, 1993; Volume 2, pp. 131–158.
2. Ball, P. *Bright Earth: Art and the Invention of Color*; Farrar, Straus and Giroux: New York, NY, USA, 2001.
3. Miguel, C.; Claro, A.; Melo, M.J.; Lopes, J.A. *Sources and Serendipity: Testimonies of Artists' Practice*; Hermens, E., Townsend, J.H., Eds.; Archetype: London, UK, 2009; pp. 33–38.
4. San Andrés, M.; Sancho, N.; Santos, S.; De La Roja, J.M. *Fatto D'archimia: Los Pigmentos Artificiales en las Técnicas Pictóricas*; Diego, C., Fominaya, M.D., Muiña, I., Eds.; Ministerio de Educación, Cultura y Deporte, Subdirección General de Documentación y Publicaciones: Madrid, Spain, 2012; pp. 197–233.
5. San Andrés, M.; De La Roja, J.M.; Santos, S.; Sancho, N. *Fatto d'archimia: Los pigmentos artificiales en las técnicas pictóricas*; Diego, C., Fominaya, M.D., Muiña, I., Eds.; Ministerio de Educación, Cultura y Deporte, Subdirección General de Documentación y Publicaciones: Madrid, Spain, 2012; pp. 235–257.
6. Berg, K.J.V.D.; Hommes, M.H.V.E.; Groen, K.M.; Boon, J.J.; Berrie, B.H. *Art et chimie, la couleur: Actes du Congrès*; Paris, 16–18 September 1998; Goupy, J., Mohen, J.-P., Eds.; CNRS: Paris, France, 2000; pp. 18–21.
7. Ricciardi, P.; Pallipurath, A.; Rose, K. 'It's not easy being green': A spectroscopic study of green pigments used in illuminated manuscripts. *Anal. Methods* **2013**, *5*, 3819–3824. [[CrossRef](#)]
8. Gilbert, B.; Denoël, S.; Weber, G.; Allart, D. Analysis of green copper pigments in illuminated manuscripts by micro-Raman spectroscopy. *Analyst* **2003**, *10*, 1213–1217. [[CrossRef](#)] [[PubMed](#)]
9. Araújo, A.R. Os Livros de Horas (séc. XV) na coleção do Palácio Nacional de Maфра: Estudo e conservação. Master's Thesis, NOVA University Lisbon, Lisbon, Portugal, 2012.
10. Salvadó, N.; Pradell, T.; Pantos, E.; Papiz, M.Z.; Molera, J.; Seco, M.; Vendrell-Saz, M.J. Identification of copper-based green pigments in Jaume Huguet's Gothic altarpieces by Fourier transform infrared microspectroscopy and synchrotron radiation X-ray diffraction. *Synchrotron Rad.* **2002**, *9*, 215–222. [[CrossRef](#)]
11. Salvadó, N.; Butí, S.; Cotte, M.; Cinque, G.; Pradell, T. Shades of green in 15th century paintings: Combined microanalysis of the materials using synchrotron radiation XRD, FTIR and XRF. *Appl. Phys. A* **2013**, *111*, 47–57. [[CrossRef](#)]
12. Knipe, P.; Eremin, K.; Walton, M.; Babini, A.; Rayner, G. Materials and techniques of Islamic manuscripts. *Herit. Sci.* **2018**, *6*, 55. [[CrossRef](#)]
13. Naumova, M.M.; Pisareva, S.A.; Nechiporenko, G.O. Green copper pigments of old Russian frescoes. *Stud. Conserv.* **1990**, *35*, 81–88.
14. Naumova, M.M.; Pisareva, S.A. A note on the use of blue and green copper compounds in paintings. *Stud. Conserv.* **1994**, *39*, 277–283.
15. Hofmann, C.; Hartl, A.; Ahn, K.; Druceikaite, K.; Henniges, U.; Potthast, A. Stabilization of Verdigris. *J. Pap. Conserv.* **2016**, *17*, 88–99. [[CrossRef](#)]
16. Kolar, J.; Strlič, M. *Iron–gall Inks: On Manufacture, Characterization, Degradation and Stabilization*; National and University Library: Ljubljana, Slovenia, 2006; p. 25.
17. Ahn, K.; Hofmann, C.; Horsky, M.; Potthast, A. How copper corrosion can be retarded—New ways investigating a chronic problem for cellulose in paper. *Carbohydr. Polym.* **2015**, *134*, 136–143. [[CrossRef](#)]
18. Hofmann, C.; Hartl, A.; Ahn, K.; Faerber, I.; Henniges, U.; Potthast, A. Studies on the Conservation of Verdigris on Paper. *Restaurator* **2015**, *36*, 147–182. [[CrossRef](#)]
19. Leygraf, C.; Wallinder, I.O.; Tidblad, J.; Graedel, T. *Atmospheric Corrosion*, 2nd ed.; John Wiley & Sons: Hoboken, NJ, USA, 2016.
20. López-Delgado, A.; Díaz, E.C.; Rull, J.M.B.; López, F.A. A Laboratory Study of the Effect of Acetic Acid Vapor on Atmospheric Copper Corrosion. *J. Electrochem. Soc.* **1998**, *145*, 4140–4147. [[CrossRef](#)]
21. López-Delgado, A.; Díaz, E.C.; Rull, J.M.B.; López, F.A. A comparative study on copper corrosion originated by formic and acetic acid vapours. *J. Mater. Sci.* **2001**, *36*, 5203–5211. [[CrossRef](#)]
22. Leygraf, C.; Hedberg, J.; Qiu, P.; Gil, H.; Henriquez, J.; Johnson, C.M. 2007 W.R. Whitney Award Lecture: Molecular in Situ Studies of Atmospheric Corrosion. *Corrosion* **2007**, *63*, 715–721. [[CrossRef](#)]

23. Chang, T.; Wallinder, I.O.; De la Fuente, D.; Chico, B.; Morcillo, M.; Welter, J.-M.; Leygraf, C. Analysis of Historic Copper Patinas. Influence of Inclusions on Patina Uniformity. *Materials* **2017**, *10*, 298. [[CrossRef](#)] [[PubMed](#)]
24. Frost, R.L.; Martens, W.N.; Kloprogge, J.T.; Williams, P.A. Raman spectroscopy of the basic copper chloride minerals atacamite and paratacamite: Implications for the study of copper, brass and bronze objects of archaeological significance. *J. Raman Spectrosc.* **2002**, *33*, 801–806. [[CrossRef](#)]
25. Drozdowski, P.; Brozyna, A. Metal isotope and density functional study of the tetracarboxylatodicopper(II) core vibrations. *Spectrochim. Acta A Mol. Biomol. Spectrosc.* **2005**, *62*, 703–710. [[CrossRef](#)] [[PubMed](#)]
26. Chaplin, T.D.; Clark, R.J.H.; Scott, A. Study by Raman microscopy of nine variants of the green-blue pigment verdigris. *J. Raman Spectrosc.* **2006**, *37*, 223–229. [[CrossRef](#)]
27. Musumeci, A.; Frost, R.L. A spectroscopic and thermoanalytical study of the mineral hoganite. *Spectrochim. Acta A Mol. Biomol. Spectrosc.* **2007**, *67*, 48–57. [[CrossRef](#)]
28. San Andrés, M.; Roja, J.M.; Baonza, V.G.; Sancho, N. Verdigris pigment: A mixture of compounds. Input from Raman spectroscopy. *J. Raman Spectrosc.* **2010**, *41*, 1468–1476. [[CrossRef](#)]
29. Coccato, A.; Bersani, D.; Coudray, A.; Sanyova, J.; Moens, L.; Vandenberghe, P. Raman spectroscopy of green minerals and reaction products with an application in Cultural Heritage research. *J. Raman Spectrosc.* **2016**, *47*, 1429–1443. [[CrossRef](#)]
30. Frost, R.L.; Williams, P.A.; Martens, W.; Leverett, P.; Kloprogge, J.T. Raman spectroscopy of basic copper (II) and some complex copper (II) sulfate minerals: Implications for hydrogen bonding. *Am. Mineral.* **2004**, *89*, 1130–1137. [[CrossRef](#)]
31. Hayez, V.; Costa, V.; Guillaume, J.; Terry, H.; Hubin, A. Micro Raman spectroscopy used for the study of corrosion products on copper alloys: Study of the chemical composition of artificial patinas used for restoration purposes. *Analyst* **2005**, *130*, 550–556. [[CrossRef](#)] [[PubMed](#)]
32. D'Antonio, M.C.; Palacios, D.; Coggiola, L.; Baran, E.J. Vibrational and electronic spectra of synthetic moolooite. *Spectrochim. Acta A Mol. Biomol. Spectrosc.* **2007**, *68*, 424–426. [[CrossRef](#)] [[PubMed](#)]
33. Castro, K.; Sarmiento, A.; Martínez-Arkarazo, I.; Madariaga, J.M.; Fernández, L.A. Green Copper Pigments Biodegradation in Cultural Heritage: From Malachite to Moolooite, Thermodynamic Modeling, X-ray Fluorescence, and Raman Evidence. *Anal. Chim.* **2008**, *80*, 4103–4110. [[CrossRef](#)] [[PubMed](#)]
34. Nevin, A.; Melia, J.L.; Osticioli, I.; Gautier, G.; Colombini, M.P. The identification of copper oxalates in a 16th century Cypriot exterior wall painting using micro FTIR, micro Raman spectroscopy and Gas Chromatography-Mass Spectrometry. *J. Cult. Herit.* **2008**, *9*, 154–161. [[CrossRef](#)]
35. Nakamoto, K. *Infrared and Raman Spectra of Inorganic and Coordination Compounds, Theory and Applications in Inorganic Chemistry*, 6th ed.; Wiley-Interscience: Hoboken, NJ, USA, 2009.
36. Buti, D.; Rosi, F.; Brunetti, B.G.; Miliani, C. In-situ identification of copper-based green pigments on paintings and manuscripts by reflection FTIR. *Anal. Bioanal. Chem.* **2013**, *405*, 2699–2711. [[CrossRef](#)]
37. Monico, L.; Rosi, F.; Miliani, C.; Daveri, A.; Brunetti, B.G. Non-invasive identification of metal-oxalate complexes on polychrome artwork surfaces by reflection mid-infrared spectroscopy. *Spectrochim. Acta A* **2013**, *116*, 270–280. [[CrossRef](#)]
38. Švarcová, S.; Hradil, D.; Hradilová, J.; Kočí, E.; Bezdička, P. Micro-analytical evidence of origin and degradation of copper pigments found in Bohemian Gothic murals. *Anal. Bioanal. Chem.* **2009**, *395*, 2037–2050. [[CrossRef](#)]
39. Lluveras, A.; Bouleard, S.; Andreotti, A.; Vendrell-Saz, M. Degradation of azurite in mural paintings: Distribution of copper carbonate, chlorides and oxalates by SRFTIR. *Appl. Phys. A* **2010**, *99*, 363–375. [[CrossRef](#)]
40. Castro, P.; Huber, M.E. *Marine Biology*, 4th ed.; McGraw-Hill: Boston, MA, USA, 2003.
41. Theophilus. *On Divers Arts: The Foremost Medieval Treatise on Painting, Glassmaking, and Metalwork*; Translated, Introduced and Annotated by John, G. Hawthorne e; Cyril Stanley Smith: Dover, UK; New York, NY, USA, 1979; pp. 35, 36, 41.
42. Strolovitch, D.L. Old Portuguese in Hebrew Script: Convention, Contact, and Convivência. Ph.D. Thesis, Department of Linguistics, Cornell University, Cornell, WI, USA, 2005; pp. 40, 141.
43. Clarke, M. *Mediaeval Painters' Materials and Techniques: The Montpellier Liber Diversarum arcium*; Archetype: London, UK, 2011; p. 112.

44. Merrifield, M.P. *Medieval and Renaissance Treatises on the Arts of Painting: Original Texts with English Translations*; Dover: Mineola, NY, USA, 2013; pp. 273, 706.
45. Bojar, H.-P.; Walter, F.; Baumgartner, J.; Farber, G. Ammineite, $\text{CuCl}_2(\text{NH}_3)_2$, a New Species Containing an Ammine Complex: Mineral Data and Crystal Structure. *Can. Mineral.* **2010**, *48*, 1359–1371. [[CrossRef](#)]
46. Silva, C.E.; Silva, L.P.; Edwards, H.G.M.; Oliveira, L.F.C. Diffuse reflection FTIR spectral database of dyes and pigments. *Anal. Bioanal. Chem.* **2006**, *386*, 2183–2191. [[CrossRef](#)] [[PubMed](#)]
47. Schrader, I.; Wittig, L.; Richter, K.; Vieker, H.; Beyer, A.; Gölzhäuser, A.; Hartwig, A.; Swiderek, P. Formation and structure of copper(II) oxalate layers on carboxy-terminated self-assembled monolayers. *Langmuir* **2014**, *30*, 11945–11954. [[CrossRef](#)] [[PubMed](#)]
48. Chukanov, N.V. *Infrared Spectra of Mineral Species: Extended Library*; Springer: Dordrecht, The Netherlands; Heidelberg, Germany; New York, NY, USA; London, UK, 2014.
49. Frost, R.L.; Yang, J.; Ding, Z. Raman and FTIR spectroscopy of natural oxalates: Implications for the evidence of life on Mars. *Chin. Sci. Bull.* **2003**, *48*, 1844–1852. [[CrossRef](#)]
50. Edwards, H.G.M.; Farwell, D.W.; Rose, S.J.; Smith, D.N. Vibrational spectra of copper (II) oxalate dihydrate, $\text{CuC}_2\text{O}_4 \cdot 2\text{H}_2\text{O}$, and dipotassium bis-oxalato copper (II) tetrahydrate, $\text{K}_2\text{Cu}(\text{C}_2\text{O}_4)_2 \cdot 4\text{H}_2\text{O}$. *J. Mol. Struct.* **1991**, *249*, 233–243. [[CrossRef](#)]
51. Clarke, R.M.; Williams, I.R. Moolooite, a naturally occurring hydrated copper oxalate from Western Australia. *Mineral. Mag.* **1986**, *50*, 295–298. [[CrossRef](#)]
52. Martens, W.N.; Frost, R.L.; Williams, P.A. Raman and infrared spectroscopic study of the basic copper chloride minerals—Implications for the study of the copper and brass corrosion and “bronze disease”. *Neues Jahrbuch für Mineralogie-Abhandlungen* **2003**, *178*, 197–215. [[CrossRef](#)]
53. Jambor, J.L.; Dutrizac, J.E.; Roberts, A.C.; Grice, J.D.; Szymanski, J.T. Clinoatacamite, a new polymorph of $\text{Cu}_2(\text{OH})_3\text{Cl}$, and its relationship to paratacamite and ‘anarakite’. *Can. Mineral.* **1996**, *34*, 61–72.
54. Braithwaite, R.S.W.; Mereiter, K.; Paar, W.H.; Clark, A.M. Herbertsmithite, $\text{Cu}_3\text{Zn}(\text{OH})_6\text{Cl}_2$, a new species, and the definition of paratacamite. *Mineral. Mag.* **2004**, *68*, 527–539. [[CrossRef](#)]
55. Liu, X.D.; Meng, D.D.; Zheng, X.G.; Hagihala, M.; Guo, Q.X. Mid-IR and Raman Spectral Properties of Clinoatacamite-Structure Basic Copper Chlorides. *Adv. Mater. Res.* **2010**, *146–147*, 1202–1205. [[CrossRef](#)]
56. Švarcová, S.; Čermáková, Z.; Hradilová, J.; Bezdička, P.; Hradil, D. Non-destructive micro-analytical differentiation of copper pigments in paint layers of works of art using laboratory-based techniques. *Spectrochim. Acta A Mol. Biomol. Spectrosc.* **2014**, *132*, 514–525. [[CrossRef](#)]
57. Banik, G. Discoloration of Green Copper Pigments in Manuscripts and Works of Graphic Art. *Restaurator* **1989**, *10*, 61–73. [[CrossRef](#)]
58. Scott, D.A.; Taniguchi, Y.; Koseto, E. The verisimilitude of verdigris: A review of the copper carboxylates. *Rev. Conserv.* **2001**, *2*, 73–91.
59. Scott, D.A. *Copper and Bronze in Art: Corrosion, Colorants, Conservation*; Getty Conservation Institute: Los Angeles, CA, USA, 2002.
60. Cariati, F.; Rampazzi, L.; Toniolo, L.; Pozzi, A. Calcium Oxalate Films on Stone Surfaces: Experimental Assessment of the Chemical Formation. *Stud. Conserv.* **2000**, *45*, 180–188.
61. Salvadó, N.; Butí, S.; Nicholson, J.; Emerich, H.; Labrador, A.; Pradell, T. Identification of reaction compounds in micrometric layers from gothic paintings using combined SR-XRD and SR-FTIR. *Talanta* **2009**, *79*, 419–428. [[CrossRef](#)] [[PubMed](#)]
62. Benner, S.A.; Devine, K.G.; Matveeva, L.N.; Powell, D.H. The missing organic molecules on Mars. *Proc. Natl. Acad. Sci. USA* **2000**, *97*, 2425–2430. [[CrossRef](#)]
63. Otero, V.; Vilarigues, M.; Carlyle, L.; Cotte, M.; De Nolf, W.; Melo, M.J. A little key to oxalate formation in oil paints: Protective patina or chemical reactor? *Photochem. Photobiol. Sci.* **2018**, *17*, 266–270. [[CrossRef](#)] [[PubMed](#)]
64. Miguel, C. *Le vert et le Rouge: A Study on the Materials, Techniques and Meaning of the Green and Red Colours in Medieval Portuguese Illuminations*. Ph.D. Dissertation, NOVA University Lisbon, Lisbon, Portugal, 2012.
65. Melo, M.J.; Araújo, R.; Castro, R.; Casanova, C. Colour degradation in medieval manuscripts. *Microchem. J.* **2016**, *124*, 837–844. [[CrossRef](#)]
66. Bernard, M.C.; Joiret, S. Understanding corrosion of ancient metals for the conservation of cultural heritage. *Electrochim. Acta* **2009**, *54*, 5199–5205. [[CrossRef](#)]

67. Colombari, P.; Tournié, A.; Maucuer, M.; Meynard, P. On-site Raman and XRF analysis of Japanese/Chinese bronze/brass patina—The search for specific Raman signatures. *J. Raman Spectrosc.* **2012**, *43*, 799–808. [[CrossRef](#)]
68. Ropret, P.; Kosec, T. Raman investigation of artificial patina on recent bronze—Part I: Climatic chamber exposure. *J. Raman Spectrosc.* **2012**, *43*, 1578–1586. [[CrossRef](#)]
69. Bongiorno, V.; Campodonico, S.; Caffara, R.; Piccardo, P.; Carnasciali, M.M. Micro-Raman spectroscopy for the characterization of artistic patinas produced on copper-based alloys. *J. Raman Spectrosc.* **2012**, *43*, 1617–1622. [[CrossRef](#)]
70. Clarke, M. *Middle English Recipes for Painters, Stainers, Scribes and Illuminators*; Oxford University Press: Oxford, UK, 2016.
71. Dinnebier, R.E.; Fischer, A.; Eggert, G.; Runčevski, T.; Wahlberg, N. X-ray Powder Diffraction in Conservation Science: Towards Routine Crystal Structure Determination of Corrosion Products on Heritage Art Objects. *J. Vis. Exp.* **2016**, *112*, 54109. [[CrossRef](#)] [[PubMed](#)]
72. Bette, S.; Kremer, R.K.; Eggert, G.; Dinnebier, R.E. On verdigris, part II: Synthesis of the 2-1-5 phase, $\text{Cu}_3(\text{CH}_3\text{COO})_4(\text{OH})_2 \cdot 5\text{H}_2\text{O}$, by long-term crystallisation from aqueous solution at room temperature. *Dalton Trans.* **2018**, *47*, 8209–8220. [[CrossRef](#)] [[PubMed](#)]



© 2019 by the authors. Licensee MDPI, Basel, Switzerland. This article is an open access article distributed under the terms and conditions of the Creative Commons Attribution (CC BY) license (<http://creativecommons.org/licenses/by/4.0/>).